Nikolic, M. R.; Minic, S.; Macvanin, M.; Stanic-Vucinic, D.; Cirkovic Velickovic, T. Analytical Protocols in Phycobiliproteins Analysis. In *Pigments from Microalgae Handbook*; Jacob-Lopes, E., Queiroz, M. I., Zepka, L. Q., Eds.; Springer International Publishing: Cham, 2020; pp 179–201. https://doi.org/10.1007/978-3-030-50971-2_8.

Chapter 3.3 Analytical Protocols in Phycobiliproteins Analysis

Milan R. Nikolic, University of Belgrade - Faculty of Chemistry, Center of Excellence for Molecular Food Sciences and Department of Biochemistry, Belgrade, Serbia; e-mail: mnikolic@chem.bg.ac.rs

Simeon Minic, University of Belgrade - Faculty of Chemistry, Center of Excellence for Molecular Food Sciences and Department of Biochemistry, Belgrade, Serbia; e-mail: sminic@chem.bg.ac.rs

Mirjana Macvanin, University of Belgrade - Faculty of Chemistry, Center of Excellence for Molecular Food Sciences, Belgrade, Serbia; e-mail: mirjana.macvanin@gmail.com

Dragana Stanic-Vucinic, University of Belgrade - Faculty of Chemistry, Center of Excellence for Molecular Food Sciences and Department of Biochemistry, Belgrade, Serbia; e-mail: dstanic@chem.bg.ac.rs

Tanja Cirkovic Velickovic, University of Belgrade - Faculty of Chemistry, Center of Excellence for Molecular Food Sciences and Department of Biochemistry, Belgrade, Serbia; Serbian Academy of Sciences and Arts, Belgrade, Serbia; Ghent University Global Campus, Incheon, South Korea; Faculty of Bioscience Engineering, Ghent University, Ghent, Belgium; e-mail: tcirkov@chem.bg.ac.rs (Corresponding author)

Abstract: The aim of this chapter is to review and discuss methodology and protocols in the analysis of phycobiliproteins (phycocyanins, allophycocyanins, and phycoerythrins) and their chromophores. Due to the presence of multiple covalently bound open-chain tetrapyrrole chromophores, phycobiliproteins are colored and strongly fluorescent molecules, with high absorption coefficients (10^5 to 10^6) and excellent fluorescent quantum yield (0.51 up to 0.98). Therefore, a vast number of methods for phycobiliproteins analysis is based on these spectral characteristics, whereas assessment of their, bioactivity is related to their exceptional redox and metal-chelating properties. This chapter is dedicated to methods used for isolation and

purification, structure analysis, physicochemical properties and stability characterization, quantification, as well as *in vitro* and *in vivo* biological activities evaluation. In addition, emerging approaches related to phycobiliproteins analysis are also reviewed including interactions with other biomolecules and ions, identification by proteomics, phycobiliprotein (chromo)peptides and computational studies of structural and dynamic properties.

Keywords: Phycobiliproteins, Phycocyanin, Allophycocyanin, Phycoerythrin, Phycocyanobilin, Chromopeptides

Introduction

Phycobiliproteins (PBPs) are a family of water-soluble, highly fluorescent bioactive molecules composed of apoproteins and phycobilin open-chain tetrapyrrole chromophores covalently bound *via* cysteine amino acid. There are three PBP classes in microalgae: phycocyanin (PC), allophycocyanin (APC) and phycoerythrin (PE), containing phycocyanobilin (PCB) and phycoerythrobilin (PEB) as pigments that differ in their spectral properties. Given its increasing application in the various fields, the aim of this chapter is to review and discuss methodology and protocols in PBPs research focusing on recent and the most relevant literature data.

PBPs isolation and purification

PBPs are produced by the photoautotrophic, mixotrophic or heterotrophic cultivation of cyanobacteria and red algae. Although recombinant production of PBPs is demanding, as a complete synthesis of PBPs depends on co-expression of α- and β-chains, in parallel with the synthesis of chromophores and their covalent attachment to protein, recombinant APC/PC were successfully produced in *E. coli* (**Chen et al. 2015a; Cherdkiatikul and Suwanwong 2014**).

Isolation of PBPs in high yield requires efficient extraction process. There are several effective approaches used for their extraction: freezing and thawing, sonication, microwave assisted extraction, pulsed electric field extraction, high-pressure homogenization, osmotic shock, acid treatment, enzymatic treatment, organic solvent extraction, etc. (reviewed in **Bleakley and**

Hayes 2017). Extraction of algal proteins could be very challenging due to the presence of mechanically robust, multilayered cell wall, and application of different polysaccharides-hydrolyzing enzymes (xylanase, cellulase, etc.) significantly increases PBPs extraction (**Dumay et al. 2013**).

Procedures for PBPs purification use single or combination of several chromatographic steps (ion-exchange chromatography, hydrophobic chromatography, gel filtration, hydroxyapatite chromatography, and expanded bed adsorption chromatography), as well as preparative electrophoresis or two-phase aqueous extraction **(Sonani et al. 2016)**. One of the main challenges during the purification of PBPs is the separation of individual PBP from PBPs mixture because of their similar properties (pI, molecular mass, chromophore spectral properties). Recently, ultrasound assisted three-phase partitioning was employed for efficient extraction and purification of PC from *Arthrospira platensis* (**Zhang et al. 2017b**).

PBPs purity is evaluated using the ratio between absorbance in the visible region (652 nm, 620 nm, 565 nm or 540 nm for APC, PC, R-PE, and B-PE, respectively) and the absorbance at 280 nm. PC preparations with $A_{620}/A_{280} > 0.7$ are considered as food grade, while those with $A_{620}/A_{280} > 4.0$ have an analytical grade of purity (**Vernès et al. 2015**). Absorbance ratio $A_{652}/A_{280} > 4.0$ means analytical purity grade of APC (**Yan et al. 2011**) whereas the commonly accepted criterion for PE purity is when A_{565}/A_{280} ratio reaches 3.2 (**Galland-Irmouli et al. 2000**). An additional approach for evaluation of PBPs purity is determination of the ratios between absorption maxima of individual PBPs. Ratio $A_{650}/A_{620}<0.3$ means that PC preparation contains negligible contamination from APC, while the ratio $A_{650}/A_{620} > 1.5$ indicates that APC is pure relatively to PC (**McGregor et al. 2008**). The purity of R-PE is also estimated by means of following indexes: $A_{565}/A_{498} \leq 1.5$ and $A_{565}/A_{620} \leq 0.005$, indicating minimal contamination by B-PE and PC, respectively (**Niu et al. 2006**). However, these absorbance ratios could sometimes give false interpretations. The pure APC in trimeric form has a peak at 652 nm, but monomers strongly absorb at 620 nm, preventing discrimination of PC from APC by visible absorption

measurements (**MacColl et al. 2003**). In these cases, other additional analytical methods, such as SDS-PAGE, are needed to obtain reliable results regarding PBPs purity. Induction of fluorescence after incubation of SDS-PAGE gels with Zn^{2+} ions specifically marks PBPs bands (**Berkelman and Lagarias 1986**), giving the possibility to make a distinction between PBP and other proteins by comparing electrophoretic gels after Zn^{2+} and CBB staining. The molecular weights of PBPs are routinely determined by gel filtration and electrophoretic techniques (SDS-PAGE and PAGE), as well as by mass spectroscopy (MS) (**Chen et al. 2006**).

Isolation of tetrapyrrole chromophores requires cleavage of thioether bond between apoprotein and bilin chromophore by acid hydrolysis, enzymatic cleavage, or extensive refluxing in alcohols. Although the most common procedure for the chromophore cleavage is still conventional reflux in methanol (**Fu et al. 1979)**, it has been shown that performing ethanolysis in the sealed vessel at 120°C decreases reaction time to 30 minutes and obtained PCB has higher purity in comparison to conventional reflux method (**Roda-Serrat et al. 2018**). Purification of released tetrapyrroles is usually performed by reversed phase HPLC (**Roda-Serrat et al. 2018**). Tetrapyrrole chromophores could also be produced recombinantly. PCB was produced in mammalian cells by metabolic engineering introducing genes for heme oxygenase-1 and PCB:ferredoxin oxidoreductase with simultaneous knock-down of biliverdin reductase A to prevent PCB reduction to phycocyanorubin (**Muller et al. 2013**).

PBPs structure and physicochemical properties evaluation

Early studies based on PBPs enzymatic or CNBr hydrolysis and products detection after Edman degradation of chromopeptides by MS, revealed that the side chain (at position 2) of tetrapyrrole ring A is covalently bound to the cysteine residues of apoprotein (**Williams and Glazer 1978**). The real progress in PBPs research has been enabled by resolving the crystal structures of several PBPs in last three decades (**Li et al. 2019**), providing valuable information about amino acid sequence(s), oligomerization state, subunit interactions, shapes of PBPs, as well as

tetrapyrrole interactions with apoproteins and chromophore conformations in binding pockets. Details about the spatial arrangement of chromophores and modulations of their conformations enabled the study of mechanisms of energy transfer between chromophores in phycobilisomes (**Jiang et al. 2001**). While X-ray crystal structures have provided molecular details on the isolated PBPs, relatively high-resolution images (3.5 Å) of the overall architecture of phycobilisome assembly were obtained by single-particle cryo-electron microscopy (**Zhang et al. 2017a**). SDS-PAGE, HPLC, and MS confirmed the existence of at least two different types of γ subunit in some PEs which exist within the central cavity of $[(\alpha\beta)_3]_2$ hexamers (**Isailovic et al. 2004; Wang et al. 2015**).

While crystallographic studies have a big impact on the understanding of the structure and function of PBPs, they do not provide answers on proteins behavior in solution. Small angle X-ray and small angle neutron scattering techniques were employed for the determination of dimensions, aggregation state and shapes of PBPs in solution (**Golub et al. 2017**). Special software (CRYSOL) was used for comparison between experimentally obtained scattering curve and theoretical curve based on the PDB file of the crystal structure of PC, enabling comparison of the structure of PBPs in crystal and solutions (**Golub et al. 2017**). PC dynamics *per se*, as well as the importance of hydration (interfacial water), have been studied by elastic incoherent neutron scattering (**Combet and Zanotti 2012**). In another approach, the structure and dynamics of chromophore binding pocket in PC were investigated by Heteronuclear Multiple-Quantum Correlation (HMQC) ^{15}N NMR. HMQC spectra unequivocally confirmed that all four nitrogen atoms of PCB in α subunit of PC are protonated (**Hahn et al. 2007**).

Optical spectroscopic properties of covalently bound tetrapyrrole chromophores alter in response to changes in conformation and oligomerization state of PBPs, which makes UV/VIS absorption, fluorescence and CD spectrometry very convenient for studying PBPs properties (**Thoren et al 2006**). An important finding is that these spectroscopic methods are useful for the characterization of PBP chromophores and their conformers in free and protein-bound form

(**Minic et al. 2015**; **Minic et al. 2018a**). Due to high absorption coefficients (10^5 to 10^6 $M^{-1}cm^1$) and excellent fluorescence quantum yields (from 0.51 to 0.98) these techniques have high sensitivity towards PBPs (**Hermanson 2013**). Based on absorption spectra, it is possible to estimate the chromophore content of PBPs and make a distinction between different PBPs. Moreover, the same chromophore molecules, bound at different sites in PBPs do not have the same spectroscopic properties, i.e. they show different absorption maxima. These differences may not be obvious in the raw absorption spectra due to broadness of peaks, but application of deconvolution method, using a Gaussian model analysis of the components, allows peaks to be resolved into several peaks that arise from the same types of chromophores bound at different regions on PBPs (**Sepúlveda-Ugarte et al. 2011**).

Study of energy transfer between tetrapyrrole chromophores during photosynthesis is an important topic in PBPs research. The energy transfers in PBPs have been investigated by steady-state fluorescence and fluorescence polarization spectroscopy, as well as by fluorescence lifetime and kinetic absorption spectroscopy (**Li et al. 2019**). Single-molecule fluorescence spectroscopy was used for analysis of switching of PC between different conformations and the role of this process in energy transmission to photosystem I (**Gwizdala et al. 2018**). UV/VIS absorption, fluorescence anisotropy, and CD spectroscopy are also useful tools for studying the effects of ionic strength, pH and protein concentration on oligomerization states of PBPs (**Thoren et al. 2006**). Additionally, analytical ultracentrifugation enables analysis of PC at smaller concentrations (≤ 0.01 mg/mL), and the determination of equilibrium constants between different oligomerization states (monomers, trimers, and hexamers) of PC (**Berns and MacColl 1989**).

PBPs quantification and stability measurements

Tetrapyrrole chromophores are responsible for the typical color of various PBPs and have characteristic light absorption properties: PE, pink-purple, λ_{max} = 540–570 nm; PC, blue, λ_{max} =

610–620 nm, and APC, bluish-green, λ_{max} = 650–655 nm (**Dufossé 2018**). The quantity of PBPs/chromophores in solution is routinely determined by measurements of absorption in the visible spectral region (usually at the wavelength(s) of PBSs maximum absorption). In general, four sets of equations, combining the extinction coefficients, are used for the estimation of PBPs concentrations. The first was described by **Bennett and Bogorad (1973)** and the concentrations are given in mg/mL:

$$[PC] = (A_{615} - 0.474\ A_{652}) / 5.34;$$

$$[APC] = (A_{652} - 0.205\ A_{615}) / 5.09;$$

$$[PE] = (A_{562} - 2.41\ [PC] - 0.849\ [APC]) / 9.62.$$

The second set was proposed by **Kursar et al. (1983)** with concentrations expressed as μg/mL:

$$[APC] = 181.3\ A_{651} - 22.3\ A_{614};$$

$$[PC] = 151.1\ A_{614} - 99.1\ A_{651};$$

$$[PE] = 155.8\ A_{498.5} - 40.0\ A_{614} - 10.5\ A_{651}.$$

For expression of the hexameric form concentration in mol/L, the authors assumed the molar mass of 210 kDa (APC), 225 kDa (PC), and 250 kDa (for PE $[(\alpha\beta)_6\gamma]$). For expression of chromophores concentration in mol/L, the number of tetrapyrroles per hexamer was assumed to be 12 (APC), 18 (PC), and 40 (for PE $[(\alpha\beta)_6\gamma]$).

Beer and Eshel (1985) proposed equations for calculation of concentration (mg/mL), which are not affected by the concentration of interfering components, and which are presently mainly used for determination of PBPs from red algae:

$$[PE] = ((A_{564} - A_{592}) - (A_{455} - A_{592})\ 0.20)\ 0.12;$$

$$[PC] = ((A_{618} - A_{645}) - (A_{592} - A_{645})\ 0.15)\ 0.15.$$

Finally, **Sampath-Wiley and Neefus (2007)** described equations for estimation of PBPs content in aqueous extracts (mg/mL), which are, according to the authors, more accurate than previously published methods:

$$[R\text{-}PC] = 0.154\ (A_{618} - A_{730});$$

$$[\text{R-PE}] = 0.1247\ ((A_{564} - A_{730}) - 0.4583\ (A_{618} - A_{730})).$$

For quantification of PCB obtained by methanolysis of purified PC, the extinction coefficient of 37900 $M^{-1}cm^{-1}$ in MeOH/HCl solution (**Cole al. 1967**) is frequently used.

While chromophore is a light-sensitive part of PBPs, apoprotein part confers the stability with respect to pH and temperature. Typically, the thermostability, the effect of pH itself or the effect of pH on thermal stability of the PBPs are measured by incubating protein samples at chosen temperatures/pH values, followed by measurements of the characteristic absorbance maximum at regular time intervals, and calculation of the remaining concentration of PBP (C_R, %) relative to the initial concentration (e.g. **Rahman et al. 2017; Wu at al. 2016; González-Ramírez et al. 2014; Liu et al. 2009**). Differences in denaturation midpoint, defined as the temperature (Tm) at which 50% of the protein still remains in solution (C_R = 50% value), the purity ratio (e.g. A_{620}/A_{280} for PC), and the half-life value ($t_{1/2}$, the time taken for the initial protein concentration to be reduced by half) are also used to compare the stability of PBPs from various algal species. The examination of conformational state and functional dynamics of PBPs by measurements of optical properties of chromophores have been recently applied to compare the stability of the full length and truncated α-subunit of cyanobacterial PE. Urea-induced denaturation α-subunit transitions were monitored and the role of the truncated region in PE stability was also investigated by molecular dynamics simulations (MDS) (**Anwer et al. 2015**).

Improving the stability of PBPs is an important goal for their practical application as natural colors in the food and cosmetic industry and as a fluorescent probe and analytical reagent (**Stanic-Vucinic et al. 2018**). PBPs spectroscopic properties, including degradation kinetics with determination of degradation rate constant (k_d), are wildly used to examine improvement of PBPs storage stability by encapsulation (**Suzery et al. 2015; Purnamayati et al. 2018**), nanofiber encapsulation and/or in the presence of preservatives (**Braga et al. 2016; Bhattacharya et al. 2018**).

Evaluation of biological activities of PBPs

The exceptional redox and metal-chelating properties of PBPs, and especially their chromophores, are proved by various biochemical assays for determination of their antioxidant potential: oxygen radical absorbance capacity (ORAC), total radical-trapping antioxidant parameter (TRAP), β-carotene or crocin bleaching, ferric ion reducing antioxidant power (FRAP), lipid peroxidation inhibition, thiobarbituric acid reactive substances (TBARS), Fe^{2+} ions chelating, copper ion reducing antioxidant capacity (CUPRAC), 1,1-diphenyl-2-picrylhydrazyl (DPPH) or 2,2'-azino-bis-(3-ethylbenzothiazoline-6-sulfonate) (ABTS) radical scavenging, hydroxyl radical absorbance capacity (HORAC), etc. (reviewed in **Kenny et al. 2015**).

An increasing number of studies, performed in different *in vivo* and *in vitro* model systems, show that purified PBPs, PBSs-enriched extracts, recombinant, and even encapsulated PBSs, as well as their chromophores, exhibit a plethora of biological activities with substantial health benefits (summarized in **Table 3.3.1**). *In vivo*, in rat, mouse and hamster models with induced disorders, PBPs were tested for their anti-cancer, anti-inflammatory, neuroprotective, nephroprotective, hepatoprotective, antihyperlipidemic and antioxidative effects, while in *Caenorhabditis elegans* PC anti-aging action was examined. *In vitro,* in healthy cells, such as human erythrocytes and rat cardiomyocytes, PBPs were examined for their protective antioxidant effects during induced oxidative stress. In cancer cell lines, anti-cancer activity of PBPs was investigated mainly by testing cell viability, cycle, and apoptosis, while mechanisms of PBS's anti-cancer action were examined by monitoring of mRNA and protein expression of genes and signaling pathways involved in cell death. Photodynamic cytotoxicity on cancer cell lines was tested upon PBPs treatment followed by laser irradiation (**Table 3.3.1**).

Table 3.3.1 Selected examples of evaluation of biological activities of PBPs *in vitro* and *in vivo.* AAPH, 2,2'-Azobis(2-amidinopropane) dihydrochloride; GOT, glutamic oxaloacetic transaminase; GPT, glutamic pyruvic transaminase; ROS, reactive oxygen species; SOD, superoxide dismutase; TNF, Tumor necrosis factor.

Disorder/disease model system	PBP source	PBP activity	Experimental approach	References
		In vivo		
Murine sarcoma 180-bearing mice	PE	Anti-cancer	Tumor inhibitory rate and organ index, SOD activity in liver and serum, splenic lymphocyte proliferation, natural killer cells activity, and TNF secretion capacity, histopathology of tumors	Pan et al. (2013)
Caenorhabditis elegans / *C. elegans* CL4176 transgenic model for Alzheimer's disease	PE	Antioxidant and anti-aging	Life span and stress resistance assays, locomotion and paralysis assays, expression of signaling pathways involved in aging; aggregation and proteotoxicity-mediated paralysis phenotype	Sonani et al. (2014a); Sonani et al. (2014b)
Acetic acid-induced colitis (Sprague-Dawley rats)	PC extract	Anti-inflammatory	Myeloperoxidase activity, histopathology and electron microscopy of colonic tissue	González et al. (1999)
Pancreatic adenocarcinoma PANC-1 based tumor xenograft (Mice)	PC	Anti-cancer	Tumor growth and weight, body weight	Liao et al. (2016)
Kainic acid-induced hippocampus neuronal damage (Sprague-Dawley rats)	PC	Neuroprotective	Neurobehavioral activities, body weight, expression of markers of microglia and astroglia	Rimbau et al. (1999)
Oxalate-induced renal injury (Wistar rats)	PC	Nephroprotective	Histopathology, oxalate content and lipid peroxidation of renal tissues, stone forming, biochemical analysis of urine	Farooq et al. (2004)
Thioacetamide - induced hepatic encephalopathy (Wistar rats)	PC	Hepatoprotective	Levels of NH_3 in serum, liver, and brain; prothrombin time and albumin levels in plasma; lipid peroxidation, Trp, antioxidant enzymes activity in the brain; histopathology and electron microscopy of brain tissue	Sathyasaikumar et al. (2007)
CCl_4 and R-(+)-pulegone-induced hepatotoxicity (Albino rats)	PC	Hepatoprotective	Serum GPT activity; liver microsomal cytochrome P450, glucose-6-phosphatase, aminopyrine-*N*-demethylase activities	Vadiraja et al. (1998)
Atherogenic diet-induced oxidative stress (Golden Syrian hamsters)	PC	Antihyperlipidemic and antioxidative	Plasma lipid concentrations and antioxidant capacity; liver antioxidant enzymes activity; aortic fatty streak area; cardiac superoxide anion production and expression of NADPH oxidase	Riss et al. (2007)
Hypercholesterolemic diet-induced hyperlipidemia and oxidative stress (Golden Syrian hamsters)	PC	Antihyperlipidemic and antioxidative	Plasma lipid concentrations, GOT/GPT activity and lipid peroxidation in serum; antioxidant enzymes activity in the liver; mRNA levels of LDL receptor, HMG-CoA reductase of HepG2 cells	Sheu et al. (2013)
Selenite-induced cataractogenesis (Wistar rat)	PC	Anticataractogenic	Antioxidant enzymes activity, lipid peroxidation, and glutathione lens tissue levels	Kumari et al. (2013)
Encephalitogen-induced autoimmune encephalomyelitis (Lewis rats)	C-PC / PCB	Anti-multiple sclerosis	Balance and motor coordination; oxidative stress markers in brain and serum; cytokine levels in the brain; electron microscopy of brain tissue	Cervantes-Llanos et al. (2018)
		In vitro		
Colon cancer	PE	Anti-cancer	Cell viability, cycle and apoptosis	Li et al.

SW480 cells			assays; electron microscopy; proteomics analysis of cell lysate; assays for signaling pathways involved in cell death	(2016)
A549 human lung carcinoma cells	PE	Anti-cancer	Cell viability, cycle and apoptosis assays; mitochondrial membrane potential and intracellular ROS generation	Madamwar et al. (2015)
Cervical carcinoma HeLa cells	PE	Anti-cancer	Cell viability and apoptosis assays after laser irradiation (photodynamic cytotoxicity); assays for signaling pathways involved in cell death	Pan et al. (2013)
Human hepatocellular carcinoma SMMC-7721 cells	PC and PE	Anti-cancer	Cell viability and apoptosis assays after laser irradiation (photodynamic cytotoxicity)	Cai et al. (2014)
AAPH-induced oxidative stress in human erythrocytes	PC-enriched algae extract	Antioxidant	Cytosolic glutathione content, lipid peroxidation, and hemolysis assay	Benedetti et al. (2004)
Pancreatic cancer Capan-1, PANC-1 and BxPC3 cell lines	PC	Anti-cancer	Cell viability, cycle, apoptosis, autophagy and autosis assays, assays for signaling pathways involved in cell death	Liao et al. (2016)
Lung cancer NCI-H1299, NCI-H460, and LTEP-A2 cell lines	PC	Anti-cancer	Cell viability, cycle, apoptosis, migration and colony formation assays; assays for signaling pathways involved in cell death	Hao et al. (2018)
Breast cancer MDA-MB-231 cell lines	PC	Anti-cancer	Cell viability, cycle, apoptosis, migration and colony formation assays; assays for signaling pathways involved in cell death	Jiang et al. (2018)
Breast cancer MDA-MB-231, MCF-7, SKBR-3, BT-474, and HBL-100 cell lines	PC	Anti-cancer and anti-angiogenic	Cell viability, cycle, apoptosis, migration and colony formation assays; angiogenic assay; assays for signaling pathways involved in cell death	Ravi et al. (2015)
Doxorubicin-induced oxidative stress in rat cardiomyocytes	PC	Cardioprotective	Cell viability and apoptosis assays; intracellular ROS generation; assays for signaling pathways involved in cell death	Khan et al. (2006)
B16F10 murine melanoma cells	PC	Anti-melanogenic	Cell viability assay, tyrosinase activity, and melanin content; assays of signaling pathways involved in melanogenesis	Wu et al. (2011)
AAPH-induced oxidative stress in human erythrocytes	Natural PC and recombinant apo-PC	Antioxidant	Hemolysis assay, electron microscopy	Pleonsil et al. (2013)
Human colon T116 cancer cell line	Encapsulated PC	Anti-cancer	Cell viability, cycle and apoptosis assays; assays for signaling pathways involved in cell death	Wen et al. (2019)

PBPs interactions with other biomolecules and ions

Although PBPs and their chromophores are prone to interact (non)covalently with other molecules and ions, there is limited literature data related to this topic. In the majority of the studies, fluorescent properties of PC and PCB are exploited for the determination of their noncovalent interactions and the most frequently used method is fluorescence quenching. In

several studies, fluorescence quenching of a chromophore was monitored upon its titration with tested molecule or ion. The interactions of PCB with proteins were also followed by fluorescence quenching of protein Trp residue(s) upon titration with PCB. **Gelagutashvili et al. (2013)** compared three methods for monitoring of heavy metal binding to PC: equilibrium dialysis, fluorescence, and absorption titration. Heavy metal binding to PC was even exploited for the creation of fluorescence chemosensor for Cu^{2+} and mercapto biomolecules (**Puangploy 2015**). Fluorescence quenching was used for monitoring of PC interactions with lectins, such as jacalin (**Pandey et al. 2009a**), concanavalin A and peanut agglutinin (**Pandey et al. 2009b**), and PCB interactions with human serum albumin (HSA) (**Minic et al. 2015**), bovine serum albumin (BSA) (**Kathiravan et al. 2009; Minic et al. 2018a**), and beta-lactoglobulin (BLG) (**Minic et al. 2018b**). For identification of PCB binding site on HSA, competition experiments with site markers, as well as the determination of binding constants in the presence of site markers were exploited (**Minic et al. 2015**). Fluorescence microscopy has shown that PC penetrates to nucleated cells and stains the nucleus. High affinity of PC for DNA was confirmed by agarose gel electrophoresis, suggesting that PC can be used as a natural non-toxic replacement for ethidium bromide for specific detection of genomic DNA and as a marker of various blood cells/molecules (**Singh et al. 2011**; **Paswan et al. 2016**). On the other hand, the microscale thermophoresis, as a new method for characterization of ligand-macromolecule binding, was used for characterization of PCB-BSA interactions (**Fig 3.3.1**; **Minic et al. 2018a**), while isothermal titration calorimetry and scanning electron microscopy-energy dispersive X-ray spectrophotometry were used for characterization of PC interactions with Hg^{2+} (**Bhayani et al. 2016**). PC interactions with lipid monolayers were investigated by surface pressure measurements (**Almog et al. 1988**). PCB interactions and its potential binding sites to proteins were also studied by molecular docking (**Minic et al. 2015**; **Minic et al. 2018a**; **Minic et al. 2018b**). Covalent binding of PCB to proteins was investigated by fluorescence and absorption spectrometry, MS and electrophoretic techniques, supported by computational methods (**Isailovic et al. 2006**; **Minic et al. 2018a**).

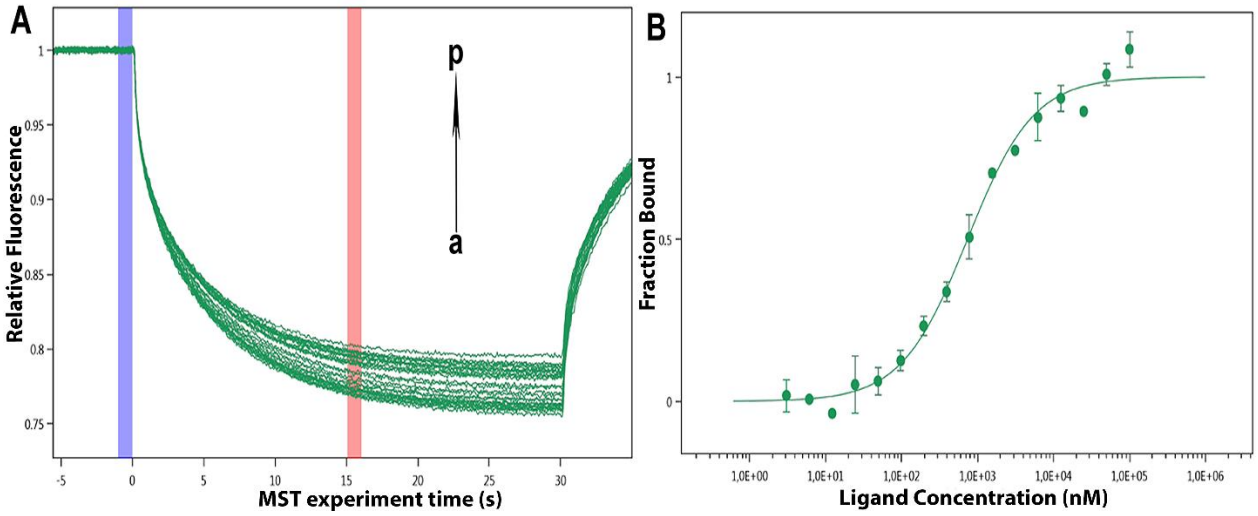

Figure 3.3.1 Microscale thermophoresis was used for the determination of PCB-BSA interactions. Reprinted from **Minic et al. (2018a**), Copyright (2018), with permission from Elsevier.

Several studies have also investigated the consequences of PC and PCB interactions with other molecules/ions on the conformation of interacting species. PCB-induced thermal stability and conformational changes of HSA, BSA, and BLG were monitored by synchronous fluorescence, CD spectroscopy, and FT-IR, while chromophore conformational changes were detected by CD spectroscopy in the visible region (**Kathiravan et al. 2009; Minic et al. 2018a; Minic et al. 2015**). Heavy metal ions-induced conformational changes of PC were observed by FT-IR and CD spectroscopy (**Bhayani et al. 2016**). The role of trehalose on the dynamics and structural stabilization of PC was investigated by neutron scattering **(Koeper et al. 2008)**. In addition, **Minic et al. (2018a)** demonstrated a mutual protective effect of complexed PCB and BSA against free radical attack using antioxidant assays.

PBPs-derived natural and synthetic (chromo)peptides

Early studies of structure and/or configuration of PBP chromophores were performed on chromopeptides and provided the means for the development of methods for their purification. **Rabier et al. (1983)** digested PC with pepsin and obtained good separation of chromopeptides on histidyl-Sepharose gels based on histidine-tetrapyrrole interactions. Chromopeptides from

pepsin digests of PC were purified by chromatography and isoelectrofocusing and, after photoisomerization, chromophore configuration was characterized by 'H NMR spectroscopy **(Thümmler and Rüdiger 1983)**. In the study of **Wedemayer et al. (1992)**, PBPs were digested by pepsin, chromopeptides were purified by chromatography, and bilin groups were identified by absorption, fluorescence, ^{1}H NMR and MS.

Although multiple studies investigated biological activities of peptides produced by enzymatic hydrolysis of whole algal biomass or isolated whole algal proteins **(Ovando et al. 2018)**, only a few of them focused on the bioactivities of (chromo)peptides obtained from purified PBPs. In several studies, in addition to the identification of bioactive peptides, some of the peptides were synthesized and tested for bioactivity. **Kim et al. (2018)** identified PBPs by proteomics and, based on obtained amino acid sequences, synthesized 13 PBPs-derived peptides which were tested for their anticancer activity effect *in vitro*. **Minic et al. (2016)** digested PC by pepsin in simulated gastric fluid, separated chromopeptides by chromatography, and analyzed chromopeptides by MS. Sequences of chromopeptides were determined by manual *de novo* sequencing and confirmation of sequences was done by analysis of MS2 and MS3 spectra of parent ions and pure PCB. They also tested chromopeptides for antioxidant and metal-chelating activities, as well as for the protection of human erythrocytes from free radical-induced hemolysis and cytotoxic effect on HeLa and Caco-2 cells. **Oh et al. (2018)** separated whole algal proteins on 2D PAGE, digested PE band by trypsin, and after identification by MS, synthesized PYP peptide and tested its effect in hippocampal neuron cell culture. **Wu et al. (2017)** hydrolyzed PE by pepsin and purified the hydrolysate by gel permeation and reversed-phase chromatography. Two peptides with the highest angiotensin-converting enzyme inhibitory activity were determined with the Edman degradation method, followed by the synthesis of peptides with the same sequences. **Xu et al. (2018)** generated PC-derived peptides by limited trypsin hydrolysis, grafted hydrolysate to N-succinyl chitosan by microbial transglutaminase and tested them for antioxidant and anticancer activity on HeLa and L929 mouse fibroblast cell lines.

PBPs identification by proteomics

Using emerging proteomic methodologies, the most recent studies used global, and especially differential proteomic analysis of cyanobacteria/algae, for investigation of their circadian rhythm, cellular differentiation or acclimation to external/stress factors and starvation focusing on the expression of PBPs. Proteomics was used to investigate the link between light adaptation responses and phylogeny (different strains) and pigmentation (different PBPs ratio) (**Mackey et al. 2017**), as well as to monitor photo-acclimation by proteomics identification of expressed genes for PBPs (**Herrera-Salgado et al. 2018**). PBPs degradation was followed by proteomics analysis during an organism's adaptation to nitrogen depletion (**Deschoenmaeker et al. 2014**) and desiccation/rehydration (**Xu et al. 2016**). In an attempt to understand the toxicity of herbicide butachlor, a proteomic approach was helpful for detection of butachlor-induced down-regulation of PBPs (**Kumari et al. 2009**). Semiquantitative proteomics was used to monitor the expression level of each of 20 PE subunits, depending on light intensity during algal growth (**Kieselbach et al. 2018**). For quantitative proteomics, isobaric tags for relative and absolute quantitation (iTRAQ) were exploited to reveal the capacity for transfer of light energy and expression of PBPs during high-temperature stress and tolerance (**Shi et al. 2017**), as well as for monitoring of PBPs abundances in response to phosphate acclimation (**Fuszard et al. 2013**). In addition to label-free proteomics, quantitative proteomics with $^{14}N/^{15}N$-labeled proteins was used for investigation of temperature-induced remodeling of the photosynthetic machinery, where cells grown at high temperature were metabolically labeled with ^{15}N (**Nikolova et al. 2017**). Phosphoproteomics, with the additional step of phosphopeptides enrichment by TiO_2 chromatography, was exploited for detecting how phosphorylation status of PBPs affects the energy transfer and state transition of photosynthesis (**Angeleri et al. 2016; Chen et al. 2015b**). **Spat et al. (2018)** used quantitative phosphoproteomics to describe the proteomic of a dormant cyanobacterium and its dynamics during the transition to vegetative growth, in order to find the link between hyper-phosphorylation and the lifespan of PBPs during chlorosis.

On the other hand, high-resolution native mass spectrometry (NMS) which preserves noncovalent interactions, enabled better insight into the adaptation of the algal light-harvesting system to a wide range of environmental conditions *via* oligomerization of PBPs (**Eisenberg et al. 2017**). The combination of NMS and fluorescence spectroscopy was used to characterize the (dis)assembly of the PE protein complex regarding species contributing to color and highly fluorescent properties of the complex (**Leney et al. 2018**). The major challenge in working with the proteome of cyanobacteria is the high abundance of PBPs which affects the dynamic detection range and therefore suppresses the MS identification of other proteins. **Matallana-Surget et al. (2014)** successfully improved the cyanobacterial proteome coverage using 3D LC-MS/MS approach. They introduced a immobilized Cu(II)-affinity chromatography separation step to eliminate PBPs as the most abundant proteins, and therefore improved access to additional low-abundance proteins. Ultimately, complete or near-complete sequences of novel PBPs could be deduced by combined proteomics and *de novo* sequencing approaches (**Nair et al. 2018**).

Computational studies of PBPs' structural and dynamics properties

MDS and quantum mechanics/molecular mechanics (QM/MM) are valuable tools for investigation of PBPs and their chromophores. These methods are useful for explanation of spectroscopic and structural properties found by experimental data, in addition to uncovering still controversial molecular mechanisms of energy transport in light-harvesting complexes. Several studies applied MDS to uncover the effects of bound solvent molecules on the conformation of PCB and dynamic of PC (**Adir et al. 2002; Bellissent-Funel 2004**). **Waterman et al. (2014)** investigated the conformational response of PCB to the ability of solvents to form hydrogen bonds using *ab initio* MDS of PCB in different solvents and *ab initio* calculations of NMR chemical shift patterns. In order to understand long-lived quantum coherences in PE, MDS, combined with quantum chemistry calculations, was employed to study the coupling between the biological environment and the vertical excitation energies of chromophores of PE antenna

system (**Aghtar et al. 2014**). MDS was exploited for monitoring of PCB conformational changes and HSA overall and individual domain flexibility upon PCB binding to any of the two found binding sites on the protein. MDS enabled refining these binding sites and supported experimental data which demonstrate PCB-induced stabilization of HSA (**Radibratovic et al. 2016**). MDS was a tool for comparison of conformational flexibility of PC from Arctic cyanobacterial strain and mesophilic *Arthrospira platensis* in relation to cold adaptation (**Su et al. 2017**). The solvation dynamics of individual pigments in PC was quantified using *ab initio* QM/MM nuclear dynamics (**Blau et al. 2018**), demonstrating how the molecular motion of PBP antennae funnel excitations to low-energy pigments. QM/MM method was established for calculating the Raman spectra of protein-bound chromophores and revealed the potential and limitations of QM calculations on isolated tetrapyrroles for determining the chromophore structures which are not available (**Mroginski et al. 2007**). **Elgabarty et al. (2013)** presented hybrid *ab initio* QM/MM MDS and theoretical NMR chemical shift calculations of PCB in the binding pocket of the α-subunit of PC, unraveling the existence of dynamic water channels in light-harvesting proteins.

Conclusion: A recent increased interest in the use of PBPs for various industrial, biotechnological, pharmaceutical and clinical applications demands reliable experimental protocols for their comprehensive analysis. The overview of traditional methods, as well as the most recent experimental advances used for PBPs' analysis given in this chapter, may be useful for further scientific research of the role of PBPs in photosynthesis. In addition, it may also serve as a literature guide for assembly of analytical protocols for PBPs analysis prior to commercial and/or medical use.

Funding: This work was supported by the Ministry of Education, Science and Technological Development of the Republic of Serbia (Grant No. OI172024). The project leading to this application has received funding from the European Union's Horizon 2020 research and

innovation programme under grant agreement No 810752. The EC does not share responsibility for the content of the article.

References

Adir, N., Vainer, R., Lerner, N., 2002. Refined structure of c-phycocyanin from the cyanobacterium Synechococcus vulcanus at 1.6 angstrom: insights into the role of solvent molecules in thermal stability and co-factor structure. Biochim. Biophys. Acta, Bioenerg. 1556, 168–174.

Aghtar, M., Strumpfer, J., Olbrich, C., Schulten, K., Kleinekathofer, U., 2014. Different Types of Vibrations Interacting with Electronic Excitations in Phycoerythrin 545 and Fenna-Matthews-Olson Antenna Systems. J. Phys. Chem. Lett. 5, 3131–3137.

Almog, R., Marsilio, F., Berns, D.S., 1988. Interaction of C-phycocyanin with lipid monolayers under nitrogen and in the presence of air. Arch. Biochem. Biophys. 260, 28–36.

Angeleri, M., Muth-Pawlak, D., Aro, E.M., Battchikova, N., 2016. Study of O-Phosphorylation Sites in Proteins Involved in Photosynthesis-Related Processes in Synechocystis sp Strain PCC 6803: Application of the SRM Approach. J. Proteome Res. 15, 4638–4652.

Anwer, K., Sonani, R., Madamwar, D., Singh, P., Khan, F., Bisetty, K., Ahmad, F., Hassan, M.I., 2015. Role of N-terminal residues on folding and stability of C-phycoerythrin: simulation and urea-induced denaturation studies. J. Biomol. Struct. Dyn. 33, 121–133.

Beer, S., Eshel, A., 1985. Determining phycoerythrin and phycocyanin concentrations in aqueous crude extracts of red algae. Aust. J. Mar. Freshwat. Res. 36, 785–793.

Bellissent-Funel, M.C., 2004. Internal motions in proteins: A combined neutron scattering and molecular modelling approach. Pramana-J. Phys. 63, 91–97.

Benedetti, S., Benvenuti, F., Pagliarani, S., Francogli, S., Scoglio, S., Canestrari, F., 2004. Antioxidant properties of a novel phycocyanin extract from the blue-green alga Aphanizomenon flos-aquae. Life Sci. 75, 2353–2362.

Bennett, A., Borogad, L., 1973. Complementary chromatic adaptation in a filamentous bluegreen alga. J. Cell Biol. 58, 419–435.

Berkelman, T.R., Lagarias, J.C., 1986. Visualization of bilin-linked peptides and proteins in polyacrylamide gels. Anal. Biochem. 156, 194-201.

Berns, D.S., MacColl, R., 1989. Phycocyanin in Physical-Chemical Studies. Chem. Rev. 89, 807–825.

Bhattacharya, S., Bhayani, K., Ghosh, T., Bajaj, S., Trivedi, N., Mishra, S., 2018. Stability of phycobiliproteins using Natural Preservative ε- Polylysine (ε-PL). Ferment. Technol., 7, 149.

Bhayani, K., Mitra, M., Ghosh, T., Mishra, S., 2016. C-Phycocyanin as a potential biosensor for heavy metals like Hg2+ in aquatic systems. RSC Adv. 6, 111599–111605.

Blau, S.M., Bennett, D.I.G., Kreisbeck, C., Scholes, G.D., Aspuru-Guzik, A., 2018. Local protein solvation drives direct down-conversion in phycobiliprotein PC645 via incoherent vibronic transport. P. Natl. Acad. Sci. USA 115, E3342–E3350.

Bleakley, S., Hayes, M., 2017. Algal Proteins: Extraction, Application, and Challenges Concerning Production. Foods 6, pii: E33.

Braga, A.R.C., da Silva Figueira, F., da Silveira, J.T., de Morais, M.G., Costa, J.A.V., Kalil, V.S.J., 2016. Improvement of Thermal Stability of C-Phycocyanin by Nanofiber and Preservative Agents. J. Food Process. Preserv. 40, 1264–1269.

Cai, C., Wang, Y., Li, C., Guo, Z., Jia, R., Wu, W., Hu, Y., He, P., 2014. Purification and photodynamic bioactivity of phycoerythrin and phycocyanin from Porphyra yezoensis Ueda. J. Ocean U. China 13, 479–484.

Cervantes-Llanos, M., Lagumersindez-Denis, N., Marín-Prida, J., Pavón-Fuentes, N., Falcon-Cama, V., Piniella-Matamoros, B., Camacho-Rodríguez, H., Fernández-Massó, J.R., Valenzuela-Silva, C., Raíces-Cruz, I., Pentón-Arias, E., Teixeira, MM., Pentón-Rol, G., 2018. Beneficial effects of oral administration of C-phycocyanin and phycocyanobilin in rodent models of experimental autoimmune encephalomyelitis. Life Sci. 194, 130–138.

Chen, H., Jiang, P., Li, F., Wu, H., 2015a. Improving production of thermostable and fluorescent holo-beta-allophycocyanin by metabolically engineered Escherichia coli using response surface methodology. Prep. Biochem. Biotechnol. 45, 730–741.

Chen, T., Wong, Y.S., Zheng, W., 2006. Purification and characterization of selenium-containing phycocyanin from selenium-enriched Spirulina platensis. Phytochemistry 67, 2424–2430.

Chen, Z., Zhan, J., Chen, Y., Yang, M., He, C., Ge, F., Wang, Q., 2015b. Effects of Phosphorylation of beta subunits of phycocyanins on state transition in the model cyanobacterium Synechocystis sp. PCC 6803. Plant Cell Phys. 56, 1997–2013.

Cherdkiatikul, T., Suwanwong, Y., 2014. Production of the alpha and beta subunits of Spirulina allophycocyanin and C-phycocyanin in Escherichia coli: A comparative study of their antioxidant activities. J. Biomol. Screen. 19, 959–965.

Cole, W.J., Chapman, D.J., Siegelman, H.W., 1967. Structure of phycocyanobilin. J. Am. Chem. Soc., 89, 3643–3645.

Combet, S., Zanotti, J.M., 2012. Further evidence that interfacial water is the main "driving force" of protein dynamics: a neutron scattering study on perdeuterated C-phycocyanin. Phys. Chem. Chem. Phys. 14, 4927–4934.

Deschoenmaeker, F., Facchini, R., Leroy, B., Badri, H., Zhang, C.C., Wattiez, R., 2014. Proteomic and cellular views of Arthrospira sp. PCC 8005 adaptation to nitrogen depletion. Microbiology 160, 1224–1236.

Dufossé, L., 2018. Microbial pigments from bacteria, yeasts, fungi, and microalgae for the food and feed industries, in: Grumezescu, A., Holban, A.M. (Eds.), Natural and artificial flavoring agents and food dyes, Handbook of food bioengineering, VII, Elsevier, 113–132.

Dumay, J., Clement, N., Morancais, M., Fleurence, J., 2013. Optimization of hydrolysis conditions of Palmaria palmata to enhance R-phycoerythrin extraction. Bioresour. Technol. 131, 21–27.

Eisenberg, I., Harris, D., Levi-Kalisman, Y., Yochelis, S., Shemesh, A., Ben-Nissan, G., Sharon, M., Raviv, U., Adir, N., Keren, N., Paltiel, Y., 2017. Concentration-based self-assembly of phycocyanin. Photosynth. Res. 134, 39–49.

Elgabarty, H., Schmieder, P., Sebastiani, D., 2013. Unraveling the existence of dynamic water channels in light-harvesting proteins: alpha-C-phycocyanobilin in vitro. Chem. Sci. 4, 755–763.

Farooq, S.M., Asokan, D., Kalaiselvi, P., Sakthivel, R., Varalakshmi, P., 2004. Prophylactic role of phycocyanin: a study of oxalate mediated renal cell injury. Chem. Biol. Interact. 149, 1–7.

Fu, E., Friedman, L.F.L., Siegelman, H.W., 1979. Mass-spectral identification and purification of phycoerythrobilin and phycocyanobilin. Biochem. J. 179, 1–6.

Fuszard, M.A., Ow, S.Y., Gan, C.S., Noirel, J., Ternan, N.G., McMullan, G., Biggs, C.A., Reardon, K.F., Wright, P.C., 2013. The quantitative proteomic response of Synechocystis sp. PCC6803 to phosphate acclimation. Aquat. Biosyst. 9, 5.

Galland-Irmouli, A.V., Pons, L., Lucon, M., Villaume, C., Mrabet, N.T., Gueant, J.L., Fleurence, J., 2000. One-step purification of R-phycoerythrin from the red macroalga Palmaria palmata using preparative polyacrylamide gel electrophoresis. J. Chromatogr. B Biomed. Sci. Appl. 739, 117–123.

Gelagutashvili, E., 2013. Binding of heavy metals with C-phycocyanin: A comparison between equilibrium dialysis, fluorescence and absorption titration. Am. J. Biomed. Life Sci. 1, 12–16.

Golub, M., Combet, S., Wieland, D.C.F., Soloviov, D., Kuklin, A., Lokstein, H., Schmitt, F.J., Olliges, R., Hecht, M., Eckert, H.J., Pieper, J., 2017. Solution structure and excitation energy transfer in phycobiliproteins of Acaryochloris marina investigated by small angle scattering. Biochim. Biophys. Acta Bioenerg. 1858, 318–324.

González, R., Rodríguez, S., Romay, C., Ancheta, O., González, A., Armesto, J., Remirez, D., Merino, N., 1999. Anti-inflammatory activity of phycocyanin extract in acetic acid-induced colitis in rats. Pharmacol. Res. 39, 55–59.

González-Ramírez, E., Andújar-Sánchez, M., Ortiz-Salmerón, E., Bacarizo, J., Cuadri, C., Mazzuca-Sobczuk, T., José Ibáñez, M., Cámara-Artigas, A.M., Martínez-Rodríguez, S., 2014. Thermal and pH stability of the B-phycoerythrin from the red algae Porphyridium cruentum. Food Biophys. 9, 184–192.

Gwizdala, M., Kruger, T.P.J., Wahadoszamen, M., Gruber, J.M., van Grondelle, R., 2018. Phycocyanin: one complex, two states, Two Functions. J. Phys. Chem. Lett. 9, 1365–1371.

Hahn, J., Kuhne, R., Schmieder, P., 2007. Solution-state (15)N NMR spectroscopic study of alpha-C-phycocyanin: implications for the structure of the chromophore-binding pocket of the cyanobacterial phytochrome Cph1. Chembiochem. 8, 2249–2255.

Hao, S., Yan, Y., Li, S., Zhao, L., Zhang, C., Liu, L., Wang, C., 2018. The in vitro anti-tumor activity of phycocyanin against non-small cell lung cancer cells. Mar. Drugs 16, pii: E178.

Hermanson, G., 2013. Bioconjugate Techniques, third ed. Academic Press.

Herrera-Salgado, P., Leyva-Castillo, L.E., Rios-Castro, E., Gomez-Lojero, C., 2018. Complementary chromatic and far-red photoacclimations in Synechococcus ATCC 29403 (PCC 7335). I: The phycobilisomes, a proteomic approach. Photosynth. Res. 138, 39–56.

Isailovic, D., Li, H.W., Yeung, E.S., 2004. Isolation and characterization of R-phycoerythrin subunits and enzymatic digests. J. Chromatogr. A 1051, 119–130.

Isailovic, D., Sultana, I., Phillips, G.J., Yeung, E.S., 2006. Formation of fluorescent proteins by the attachment of phycoerythrobilin to R-phycoerythrin alpha and beta apo-subunits. Anal. Biochem. 358, 38–50.

Jiang, L., Wang, Y., Liu, G., Liu, H., Zhu, F., Ji, H, Li, B., 2018. C-Phycocyanin exerts anti-cancer effects via the MAPK signaling pathway in MDA-MB-231 cells. Cancer Cell Int. 18, 12.

Jiang, T., Zhang, J.P., Chang, W.R., Liang, D.C., 2001. Crystal structure of R-phycocyanin and possible energy transfer pathways in the phycobilisome. Biophys. J. 81, 1171-1179.

Kathiravan, A., Chandramohan, M., Renganathan, R., Sekar, S., 2009. Spectroscopic studies on the interaction between phycocyanin and bovine serum albumin. J. Mol. Struct. 919, 210–214.

Kenny, O., Brunton, N.P., Smyth, T.J., 2015. In vitro protocols for measuring the antioxidant capacity of algal extracts, in: Stengel, D., Connan, S. (Eds.), Natural products from marine algae, Methods Mol. Biol., Humana Press, New York, 1308, 375–402.

Khan, M., Varadharaj, S., Shobha, J.C., Naidu, M.U., Parinandi, N.L., Kutala, V.K., Kuppusamy, P., 2006. C-phycocyanin ameliorates doxorubicin-induced oxidative stress and apoptosis in adult rat cardiomyocytes. J. Cardiovasc. Pharmacol. 47, 9–20.

Kieselbach, T., Cheregi, O., Green, B.R., Funk, C., 2018. Proteomic analysis of the phycobiliprotein antenna of the cryptophyte alga Guillardia theta cultured under different light intensities. Photosynth. Res. 135, 149–163.

Kim, E.Y., Choi, Y.H., Nam, T.J., 2018. Identification and antioxidant activity of synthetic peptides from phycobiliproteins of Pyropia yezoensis. Int. J. Mol. Med. 42, 789–798.

Koeper, I., Combet, S., Petry, W., Bellissent-Funel, M.C., 2008. Dynamics of C-phycocyanin in various deuterated trehalose/water environments measured by quasielastic and elastic neutron scattering. Eur. Biophys. J. Biophy. 37, 739–748.

Kumari, N., Narayan, O.P., Rai, L.C., 2009. Understanding butachlor toxicity in Aulosira fertilissima using physiological, biochemical and proteomic approaches. Chemosphere 77, 1501–1507.

Kumari, R.P., Sivakumar, J., Thankappan, B., Anbarasu, K., 2013. C-phycocyanin modulates selenite-induced cataractogenesis in rats. Biol. Trace Elem. Res. 151, 59–67.

Kursar, T.A., Vander, M.J., Alberte, R.S., 1983. Light-harvesting system of the red alga Gracilaria tikvahiae. I Biochemical analysis of pigment mutations. Plant Physiol. 73, 353–360.

Leney, A.C., Tschanz, A., Heck, A.J.R., 2018. Connecting color with assembly in the fluorescent B-phycoerythrin protein complex. FEBS J. 285, 178–187.

Li, P., Ying, J., Chang, Q., Zhu, W., Yang, G., Xu, T., Yi, H., Pan, R., Zhang, E., Zeng, X., Yan, C., Bao, Q., Li, S., 2016. Effects of phycoerythrin from Gracilaria lemaneiformis in proliferation and apoptosis of SW480 cells. Oncol. Rep. 36, 3536–3544.

Li, W., Su, H.N., Pu, Y., Chen, J., Liu, L.N., Liu, Q., Qin, S., 2019. Phycobiliproteins: Molecular structure, production, applications, and prospects. Biotechnol. Adv. 37, 340–353.

Liao, G., Gao, B., Gao, Y., Yang, X., Cheng, X., Ou, Y., 2016. Phycocyanin inhibits tumorigenic potential of pancreatic cancer cells: Role of apoptosis and autophagy. Sci. Rep. 6, 34564.

Liu, L.N., Su, H.N., Yan, S.G., Shao, S.M., Xie, B.B., Chen, X.L., Zhang, X.Y., Zhou, B.C., Zhang, Y.Z., 2009. Probing the pH sensitivity of R-phycoerythrin: investigations of active conformational and functional variation. Biochim. Biophys. Acta. 1787, 939–946.

MacColl, R., Eisele, L.E., Menikh, A., 2003. Allophycocyanin: trimers, monomers, subunits, and homodimers. Biopolymers 72, 352–365.

Mackey, K.R.M., Post, A.F., McIlvin, M.R., Saito, M.A., 2017. Physiological and proteomic characterization of light adaptations in marine Synechococcus. Environ. Microbiol. 19, 2348–2365.

Madamwar, D., Patel, D.K., Desai, S.N., Upadhyay, K.K., Devkar, R.V., 2015. Apoptotic potential of C-phycoerythrin from Phormidium sp. A27DM and Halomicronema sp. A32DM on human lung carcinoma cells. EXCLI J. 14, 527–539.

Matallana-Surget, S., Derock, J., Leroy, B., Badri, H., Deschoenmaeker, F., Wattiez, R., 2014. Proteome-wide analysis and diel proteomic profiling of the cyanobacterium Arthrospira platensis PCC 8005. PLoS One 9, e99076.

McGregor, A., Klartag, M., David, L., Adir, N., 2008. Allophycocyanin trimer stability and functionality are primarily due to polar enhanced hydrophobicity of the phycocyanobilin binding pocket. J. Mol. Biol. 384, 406–421.

Minic, S., Radomirovic, M., Radibratovic, M., Milcic, M., Stanic-Vucinic, D., Nikolic, M., Cirkovic Velickovic, T., 2018a. Characterization and effects of binding of food-derived bioactive phycocyanobilin to bovine serum albumin. Food Chem. 239, 1090–1099.

Minic, S., Radomirovic, M., Savkovic, N., Radibratovic, M., Mihailovic, J., Vasovic, T., Nikolic, M., Milcic, M., Stanic-Vucinic, D., Cirkovic Velickovic, T., 2018b. Covalent binding of food-derived

blue pigment phycocyanobilin to bovine beta-lactoglobulin under physiological conditions. Food Chem. 269, 43–52.

Minic, S.L., Milcic, M., Stanic-Vucinic, D., Radibratovic, M., Sotiroudis, T.G., Nikolic, M.R., Cirkovic Velickovic, T., 2015. Phycocyanobilin, a bioactive tetrapyrrolic compound of blue-green alga Spirulina, binds with high affinity and competes with bilirubin for binding on human serum albumin. RSC Adv. 5, 61787–61798.

Minic, S.L., Stanic-Vucinic, D., Mihailovic, J., Krstic, M., Nikolic, M.R., Cirkovic Velickovic, T., 2016. Digestion by pepsin releases biologically active chromopeptides from C-phycocyanin, a blue-colored biliprotein of microalga Spirulina. J. Proteomics 147, 132–139.

Mroginski, M.A., Mark, F., Thiel, W., Hildebrandt, P., 2007. Quantum mechanics/molecular mechanics calculation of the Raman spectra of the phycocyanobilin chromophore in alpha-c-phycocyanin. Biophys. J. 93, 1885–1894.

Muller, K., Engesser, R., Timmer, J., Nagy, F., Zurbriggen, M.D., Weber, W., 2013. Synthesis of phycocyanobilin in mammalian cells. Chem. Commun. (Camb.) 49, 8970–8972.

Nair, D., Krishna, J.G., Panikkar, M.V.N., Nair, B.G., Pai, J.G., Nair, S.S., 2018. Identification, purification, biochemical and mass spectrometric characterization of novel phycobiliproteins from a marine red alga, Centroceras clavulatum. Int. J. Biol. Macromol. 114, 679–691.

Nikolova, D., Weber, D., Scholz, M., Bald, T., Scharsack, J.P., Hippler, M., 2017. Temperature-induced remodeling of the photosynthetic machinery tunes photosynthesis in the thermophilic alga Cyanidioschyzon merolae. Plant Physiol. 174, 35–46.

Niu, J.F., Wang, G.C., Tseng, C.K., 2006. Method for large-scale isolation and purification of R-phycoerythrin from red alga Polysiphonia urceolata Grev. Protein Expr. Purif. 49, 23–31.

Oh, J.H., Kim, E.Y., Nam, T.J., 2018. Phycoerythrin-derived tryptic peptide of a red Alga Pyropia yezoensis attenuates glutamate-induced ER stress and neuronal senescence in primary rat hippocampal neurons. Mol. Nutr. Food Res. 62, e1700469.

Ovando, C.A., de Carvalho, J.C., Pereira, G.V.D., Jacques, P., Soccol, V.T., Soccol, C.R., 2018. Functional properties and health benefits of bioactive peptides derived from Spirulina: A review. Food Rev. Int. 34, 34–51.

Pan, Q., Chen, M., Li, J., Wu, Y., Zhen, C., Liang, B., 2013. Antitumor function and mechanism of phycoerythrin from Porphyra haitanensis. Biol. Res. 46, 87–95.

Pandey, G., Fatma, T., Cowsik, S.M., Komath, S.S., 2009a. Specific interaction of jacalin with phycocyanin, a fluorescent phycobiliprotein. J. Photoch. Photobio. B 97, 87–93.

Pandey, G., Fatma, T., Komath, S.S., 2009b. Specific Interaction of the legume lectins, concanavalin A and peanut agglutinin, with phycocyanin. Photochem. Photobiol. 85, 1126–1133.

Paswan, M.B., Chudasama, M.M., Mitra, M., Bhayani, K., George, B., Chatterjee, S., Mishra, S., 2016. Fluorescence quenching property of C-phycocyanin from Spirulina platensis and its binding efficacy with viable cell components. J. Fluoresc. 26, 577–583.

Pleonsil, P., Soogarun, S., Suwanwong, Y., 2013. Anti-oxidant activity of holo- and apo-c-phycocyanin and their protective effects on human erythrocytes. Int. J. Biol. Macromol. 60, 393–398.

Puangploy, P., Oaew, S., Surareungchai, W., 2015. Development of fluorescent phycocyanin-Cu^{2+} chemosensor for detection of homocysteine. Int. J. Biosci. Biochem. Bioinforma. 5, 241–248.

Purnamayati, L., Dewi, E.N., Kurniasih, R.A., 2018. Phycocyanin stability in microcapsules processed by spray drying method using different inlet temperature. IOP Conf. Ser. Earth Environment. Sci. 116, 012076.

Rabier, J., Vijayalakshmi, M., 1983. Affinity of phycocyanin chromopeptides to histidyl-sepharose gels: A model for histidine-tetrapyrrol-interactions in biliproteins. Z. Naturforsch. C 38, 230–236.

Radibratovic, M., Minic, S., Stanic-Vucinic, D., Nikolic, M., Milcic, M., Cirkovic Velickovic, T., 2016. Stabilization of human serum albumin by the binding of phycocyanobilin, a bioactive

chromophore of blue-green alga Spirulina: Molecular dynamics and experimental Study. PLoS One 11, e0167973.

Rahman, D.Y., Sarian, F.D., van Wijk, A., Martinez-Garcia, M., van der Maarel, M.J.E.C., 2017. Thermostable phycocyanin from the red microalga Cyanidioschyzon merolae, a new natural blue food colorant. J. Appl. Phycol. 29, 1233–1239.

Ravi, M., Tentu, S., Baskar, G., Rohan Prasad, S., Raghavan, S., Jayaprakash, P., Jeyakanthan, J., Rayala, S.K., Venkatraman, G., 2015. Molecular mechanism of anti-cancer activity of phycocyanin in triple-negative breast cancer cells. BMC Cancer 15, 768.

Rimbau, V., Camins, A., Romay, C., González, R., Pallàs, M., 1999. Protective effects of C-phycocyanin against kainic acid-induced neuronal damage in rat hippocampus. Neurosci. Lett. 276, 75–78.

Riss, J., Décordé, K., Sutra, T., Delage, M., Baccou, J.C., Jouy, N., Brune, J.P., Oréal, H., Cristol, J.P., Rouanet, J.M., 2007. Phycobiliprotein C-phycocyanin from Spirulina platensis is powerfully responsible for reducing oxidative stress and NADPH oxidase expression induced by an atherogenic diet in hamsters. J. Agric. Food. Chem. 55, 7962–7967.

Roda-Serrat, M.C., Christensen, K.V., El-Houri, R.B., Frette, X., Christensen, L.P., 2018. Fast cleavage of phycocyanobilin from phycocyanin for use in food colouring. Food Chem. 240, 655–661.

Sampath-Wiley, P., Neefus, C., 2007. An improved method for estimating R-phycoerythrin and R-phycocyanin contents from crude aqueous extracts of Porphyra (Bangiales, Rhodophyta). J. Appl. Phycol. 19, 123–129.

Sathyasaikumar, K.V., Swapna, I., Reddy, P.V., Murthy, Ch.R., Roy, K.R., Dutta Gupta, A., Senthilkumaran, B., Reddanna, P., 2007. Co-administration of C-phycocyanin ameliorates thioacetamide-induced hepatic encephalopathy in Wistar rats. J. Neurol. Sci. 252, 67–75.

Sepúlveda-Ugarte, J., Brunet, J.E., Matamala, A.R., Martínez-Oyanedel, J., Bunster M., 2011. Spectroscopic parameters of phycoerythrobilin and phycourobilin on phycoerythrin from Gracilaria chilensis. J. Photochem. Photobiol. A 219, 211–216.

Sheu, M.J., Hsieh Y.Y., Lai, C.H., Chang, C.C., Wu, C.H., 2013. Antihyperlipidemic and antioxidant effects of C-phycocyanin in Golden Syrian hamsters fed with a hypercholesterolemic diet. J. Tradit. Complement. Med. 3, 41–47.

Shi, J., Chen, Y., Xu, Y., Ji, D., Chen, C., Xie, C., 2017. Differential proteomic analysis by iTRAQ reveals the mechanism of Pyropia haitanensis responding to high temperature stress. Sci. Rep. 7, 44734.

Singh, P., Kuddus, M., Thomas, G., 2011. Isolation and binding affinity of C-phycocyanin to blood cells and genomic DNA as well as its diagnostic applications. J. Biotech. Pharm. Res. 2, 001–008.

Sonani, R.R., Rastogi, R.P., Patel, R., Madamwar, D., 2016. Recent advances in production, purification and applications of phycobiliproteins. World J. Biol. Chem. 7, 100–109.

Sonani, R.R., Singh, N.K., Awasthi, A., Prasad, B., Kumar, J., Madamwar, D., 2014a. Phycoerythrin extends life span and health span of Caenorhabditis elegans. Age (Dordr.) 36, 9717.

Sonani, R.R., Singh, N.K., Kumar, J., Thakar, D., Madamwar, D., 2014b. Concurrent purification and antioxidant activity of phycobiliproteins from Lyngbya sp. A09DM: an antioxidant and anti-aging potential of phycoerythrin in Caenorhabditis elegans. Process. Biochem. 49, 1757–1766.

Spat, P., Klotz, A., Rexroth, S., Macek, B., Forchhammer, K., 2018. Chlorosis as a developmental program in cyanobacteria: The proteomic fundament for survival and awakening. Mol. Cell Proteomics 17, 1650–1669.

Stanic-Vucinic, D., Minic, S., Nikolic M.R., Cirkovic Velickovic, T., 2018. Spirulina phycobiliproteins as food components and complements, in: Jacob-Lopes, E., Zepka, L.Q., Queiroz, M.I. (Eds.), Microalgal biotechnology, IntechOpen, 129–149.

Su, H.N., Wang, Q.M., Li, C.Y., Li, K., Luo, W., Chen, B., Zhang, X.Y., Qin, Q.L., Zhou, B.C., Chen, X.L., Zhang, Y.Z., Xie, B.B., 2017. Structural insights into the cold adaptation of the photosynthetic pigment-protein C-phycocyanin from an Arctic cyanobacterium. Biochim Biophys Acta Bioenerg. 1858, 325–335.

Suzery, M., Hadiyanto, Sutanto, H., Soetrisnanto, D., Majid, D., Setyawan, D., Azizah, N., 2015. The improvement of phycocyanin stability extracted from Spirulina sp using extrusion encapsulation technique. AIP Conf. Proceed. 1699, 030011.

Thoren, K.L., Connell, K.B., Robinson, T.E., Shellhamer, D.D., Tammaro, M.S., Gindt, Y.M., 2006. The free energy of dissociation of oligomeric structure in phycocyanin is not linear with denaturant. Biochemistry 45, 12050–12059.

Thümmler, F., Rüdiger, W., 1983. Chromopeptides from phytochrome and phycocyanin. NMR Studies of the Pfr and Pr chromophore of phytochrome and EyZ isomeric chromophores of phycocyanin. Z. Naturforsch. C 38, 359–368.

Vadiraja, B.B., Gaikwad, N.W., Madyastha, K.M., 1998. Hepatoprotective effect of C-phycocyanin: protection for carbon tetrachloride and R-(+)-pulegone-mediated hepatotoxicity in rats. Biochem. Biophys. Res. Commun. 249, 428–431.

Vernès, L., Granvillain, P., Chemat, F., Vian., M., 2015. Phycocyanin from Arthrospira platensis. Production, extraction and analysis. Curr. Biotechn. 4, 481–491.

Wang, L., Wang, S., Fu, X., Sun, L., 2015. Characteristics of an R-phycoerythrin with two gamma subunits prepared from red macroalga Polysiphonia urceolata. PLoS One 10, e0120333.

Watermann, T., Elgabarty, H., Sebastiani, D., 2014. Phycocyanobilin in solution - a solvent triggered molecular switch. Phys. Chem. Chem. Phys. 16, 6146–6152.

Wedemayer, G.J., Kidd, D.G., Wemmer, D.E., Glazer, A.N., 1992. Phycobilins of cryptophycean algae. Occurrence of dihydrobiliverdin and mesobiliverdin in cryptomonad biliproteins. J. Biol. Chem. 267, 7315–7331.

Wen P, Hu TG, Wen Y, Linhardt RJ, Zong MH, Zou YX, Wu H., 2019. Targeted delivery of phycocyanin for the prevention of colon cancer using electrospun fibers. Food Funct. doi: 10.1039/c8fo02447b.

Williams, V.P., Glazer, A.N., 1978. Structural studies on phycobiliproteins. I. Bilin-containing peptides of C-phycocyanin. J. Biol. Chem. 253, 202–211.

Wu, H.-L., Wang, G.-H., Xiang, W.-Z., Li, T., He, H., 2016. Stability and antioxidant activity of food-grade phycocyanin isolated from Spirulina platensis. Int. J. Food Prop. 19, 2349–2362.

Wu, L.C., Lin, Y.Y., Yang, S.Y., Weng, Y.T., Tsai, Y.T., 2011. Antimelanogenic effect of c-phycocyanin through modulation of tyrosinase expression by upregulation of ERK and downregulation of p38 MAPK signaling pathways. J. Biomed. Sci. 18, 74.

Wu, Q., Cai, Q.F., Yoshida, A., Sun, L.C., Liu, Y.X., Liu, G.M., Su, W.J., Cao, M.J., 2017. Purification and characterization of two novel angiotensin I-converting enzyme inhibitory peptides derived from R-phycoerythrin of red algae (Bangia fusco-purpurea). Eur. Food Res. Technol. 243, 779–789.

Xu, K., Xu, Y., Ji, D.H., Xie, J., Chen, C.S., Xie, C.T., 2016. Proteomic analysis of the economic seaweed Pyropia haitanensis in response to desiccation. Algal Res. 19, 198–206.

Xu, W.Y., Xiao, Y., Luo, P.F., Fan, L.H., 2018. Preparation and characterization of C-phycocyanin peptide grafted N-succinyl chitosan by enzyme method. Int. J. Biol. Macromol. 113, 841–848.

Yan, S.-G., Zhu, L.-P., Su, H.-N., Zhang, X.-Y., Chen, X.-L., Zhou, B.-C., Zhang, Y.-Z., 2011. Single-step chromatography for simultaneous purification of C-phycocyanin and allophycocyanin with high purity and recovery from Spirulina (Arthrospira) platensis. J. Appl. Phycol. 23, 1–6.

Zhang, J., Ma, J., Liu, D., Qin, S., Sun, S., Zhao, J., Sui, S.F., 2017a. Structure of phycobilisome from the red alga Griffithsia pacifica. Nature 551, 57–63.

Zhang, X.-F., Wang, X., Luo, G.-H., 2017b. Ultrasound-assisted three phase partitioning of phycocyanin from Spirulina platensis. Eur. J. Pure Appl. Chem. 4, 1–15.